CHIRAL SYMMETRY AMPLITUDES IN THE S-WAVE ISOSCALAR AND ISOVECTOR CHANNELS AND THE $\sigma, f_0(980), a_0(980)$ SCALAR MESONS

J.A. Oller and E. Oset

Departamento de Física Teórica and IFIC, Centro Mixto Universidad de Valencia - CSIC, 46100 Burjassot (Valencia) Spain.

Abstract

We use a nonpertubative approach which combines coupled channel Lippmann Schwinger equations with meson-meson potentials provided by the lowest order chiral Lagrangian. By means of one parameter, a cut off in the momentum of the loop integrals, which results of the order of 1 GeV, we obtain singularities in the S-wave amplitudes corresponding to the σ, f_0 and a_0 resonances. The $\pi\pi \to \pi\pi$, $\pi\pi \to K\bar{K}$ phase shifts and inelasticities in the $T = 0$ scalar channel are well reproduced as well as the $\pi^0\eta$ and $K\bar{K}$ mass distributions in the $T = 1$ channel. Furthermore, the total and partial decay widths of the f_0 and a_0 resonances are properly reproduced including also the decay into the $\gamma\gamma$ channel. The results seem to indicate that chiral symmetry constraints at low energy and unitarity in coupled channels is the basic information contained in the meson-meson interaction below $\sqrt{s} \simeq 1.2\ GeV$.

1 Introduction

The understanding of the meson-meson interaction in the scalar sector is still problematic. There is some debate about the spectrum of hadronic states and even more about its nature. Below $\sqrt{s} = 1.2\ GeV$, which we will study here, the existence of a broad scalar-isoscalar meson around 500 MeV has had permanent ups and downs. However, the $f_0(980)$ (also called S^*, $I^G(J^{PC}) = 0^+(0^{++})$), and the $a_0(980)$ (also called δ, $I^G(J^{PC}) = 1^-(0^{++})$) mesonic states are well established experimentally, although there is still debate around their decay widths and particularly about their nature. Following the discovery of the f_0 [1], and a_0 [2], several proposals were made about the nature of these states: $q\bar{q}$ states [3–10], multiquark states [11, 12] or $K\bar{K}$ molecules [13, 14, 15, 16]. Other works argue against the $q\bar{q}$ nature of the states [17]. It is also interesting to investigate the structure of these states in order to better isolate possible candidates for glueballs and other states rich in gluons. For instance, in ref. [18] a glueball state at 992 MeV ($S_1(991)$) is predicted in addition to the $f_0(980)$ and the σ which have another nature. In ref. [19] a glueball at energies below 0.7 GeV is also predicted which could be a candidate for the σ. However, its narrow width around 60 MeV is considerably smaller than the 400 MeV associated to the conventional σ width in the $\pi\pi$ interaction. On the other hand in more recent calculations [20] the states with a significant component of gluons are only predicted at energies around 1.5 GeV or higher.

The situation in the scalar sector contrasts with the vector and tensor sector where the constituent quark models are rather successful in the interpretation of the spectrum and properties of the particles.

Coming back to the meson-meson interaction in the scalar sector, a large fraction of the work done consists in a parametrization of the amplitudes respecting general principles [4, 5, 6, 7, 21] while some other works use models inspired in QCD [11, 12, 13, 14, 15] or phenomenological ones based on the exchange of mesons [16].

Along the lines of the amplitude parametrization it is interesting to quote the work of [22, 23] where it is shown that one pole close to a strong threshold (*f.i.* $K\bar{K}$) in the II Riemann sheet (we follow the notations of ref. [24]) indicates the presence of a molecular state resulting from the forces between the participant mesons ($K\bar{K}, \pi\pi$ in $T = 0$ or $K\bar{K}, \eta\pi$ in $T = 1$). Conversely, the presence of two poles close to threshold, one in the II sheet and another one in the IV sheet, would indicate a $q\bar{q}$ state. The analysis in ref. [5, 6, 7] favours this latter interpretation, but in ref. [21] the first interpretation is advocated, since the pole found in the IV sheet is far from threshold. Following this debate, in ref. [7] it is argued that the $J/\psi \to \phi\pi\pi, \phi K\bar{K}$ decay is crucial in order to distinguish between the two interpretations quoted above, questioning the conclusions of [21] and offering a good description of these data. However, in ref. [16] the f_0, appears as a pole in the II sheet and a description of the $J/\psi \to \phi\pi\pi, \phi K\bar{K}$ data of the same quality as in [7] is obtained. The main sources of discrepancy between [7] and [21] come from the different ways in which the background is treated.

Among of the QCD inspired models, in refs. [11, 12] the $q^2\bar{q}^2$ states in a bag model is discussed and a rich spectrum of $SU(3)$ multiplets is obtained which would

accommodate the σ, f_0, a_0 mesons in a same nonet. On the other hand the work in ref. [13, 14, 15] starts from a colour confining Hamiltonian with hyperfine interaction and studies the same $q^2\bar{q}^2$ system. According to this latter work the rich spectrum predicted in ref. [11] disappears because the states separate into colour singlets, exception made of two weakly bound $K\bar{K}$ states with $T = 0$ and $T = 1$ which are identified as the f_0 and a_0 respectively (the authors also warn about the influence in such states of other meson-meson components due to the coupling of different channels).

In ref. [8, 9] the authors use a unitarized version of the quark model and conclude the existence of a σ and also that the f_0, a_0 are manifestations of $\bar{s}\bar{s}$ and $q\bar{q}$ states respectively, although they spend most of their time as $K\bar{K}$ components.

In ref. [16] the Jülich meson exchange model [25] is extended to account for the meson-meson interaction in the $T = 0$ and $T = 1$ channels. A coupled channel approach with the $K\bar{K}$ and $\pi\pi$ channel in $T = 0$ and $K\bar{K}$ and $\pi\eta$ channel in $T = 1$ was followed and the f_0 and a_0 states appeared as poles of the t-matrix.

The different approaches which are successful in reproducing the meson-meson scattering amplitudes rely upon a relatively high number of parameters which are adjusted to the data, and vary between around 25 in [4, 5, 6, 7, 21] and 5-6 in [8, 15].

One of the properties which has been used to discriminate among models is the $\gamma\gamma$ decay width of the f_0, a_0 states [26], and typically has been presented as a support for the $K\bar{K}$ molecule nature of the f_0 and a_0 states [27]. However, the experimental errors are still relatively high and the data can be accommodated in several models. A brief summary of the present situation in the scalar sector can be found in ref. [28].

Another different approach to the meson-meson scattering is chiral perturbation theory [29, 30, 31, 32].

Calculations have been carried out to one loop and one needs counterterms which require the use of 10 parameters fitted to experimental data. The approach is valid at energies below $600 - 700\ MeV$ but such as the perturbative calculations are carried out they show obvious limitations to face the singularities in the t matrix.

From the former discussion we can see that a key ingredient in most of the models which successfully describe the amplitudes in the $L = 0, T = 0, 1$ sector is the solution of coupled channel scattering equations starting from some potential [15, 16, 33]. On the other hand the success of chiral perturbation theory as an alternative approach to the dynamics of QCD, using mesonic instead of quark degrees of freedom, makes the use of the chiral Lagrangian extremely appealing. The combination of these two factors is the main contribution of the present work. In this sense similar steps in the baryon-meson sector have been done in refs. [34, 35] with a remarkable success. We shall see that this is also the case here. Our model accounts automatically for unitary and analyticity and leads to poles in the scattering matrix for the σ, f_0 and a_0 states below $\sqrt{s} = 1.2\ GeV$. It predicts the mass and partial decay widths of the f_0 and a_0 resonances, as well as the different scattering amplitudes, in good agreement with experiment and requires the use of only one parameter which is a cut off in the loop integrations, following also the spirit of the approach of refs. [34, 35]. This cut off is around $1.2\ GeV$, very close to the value of the scale of chiral symmetry breaking, Λ_χ [36], which plays the similar role as a scale of energies as our cut off.

2 $L = 0, T = 0, 1$ strong amplitudes in lowest order of chiral perturbation theory

.

We start from the standard chiral Lagrangian in lowest order of chiral perturbation theory (χPT) $\mathcal{L}_2$ which contains the most general low energy interactions of the pseudoscalar meson octet [29–32] in this order. This Lagrangian will provide the potentials which will be used in the coupled channel scattering equations. The interaction chiral Lagrangian is given by

$$\mathcal{L}_2 = \frac{1}{12f^2} < (\partial_\mu \Phi\Phi - \Phi\partial_\mu\Phi)^2 + M\Phi^4 > \tag{1}$$

where the symbol $<>$ indicates the trace in the flavour space of the $SU(3)$ matrices appearing in Φ and M, f is the pion decay constant and the matrices Φ and M are given by

$$\Phi \equiv \frac{\vec{\lambda}}{\sqrt{2}}\vec{\phi} = \begin{pmatrix} \frac{1}{\sqrt{2}}\pi^0 + \frac{1}{\sqrt{6}}\eta_8 & \pi^+ & K^+ \\ \pi^- & -\frac{1}{\sqrt{2}}\pi^0 + \frac{1}{\sqrt{6}}\eta_8 & K^0 \\ K^- & \bar{K}^0 & -\frac{2}{\sqrt{6}}\eta_8 \end{pmatrix}$$

$$M \begin{pmatrix} m_\pi^2 & 0 & 0 \\ 0 & m_\pi^2 & 0 \\ 0 & 0 & 2m_K^2 - m_\pi^2 \end{pmatrix} \tag{2}$$

where in M we have taken the isospin limit ($m_u = m_d$). From eqs. (1) and (2) we can write the tree level amplitudes for $K\bar{K}, \pi\pi$ and $\pi\eta$ (we take $\eta \equiv \eta_8$)

$$\begin{aligned} &\text{a)} \quad K^+(k)K^-(p) \to K^+(k')K^-(p') \\ &\quad t_a = -\tfrac{1}{3f^2}(s + t - 2u + 2m_K^2) \end{aligned} \tag{3}$$

$$\begin{aligned} &\text{b)} \quad K^0(k)\bar{K}^0(p) \to K^0(k')\bar{K}^0(p') \\ &\quad t_b = t_a \end{aligned} \tag{4}$$

$$\begin{aligned} &\text{c)} \quad K^+(k)K^-(p) \to K^0(k')\bar{K}^0(p') \\ &\quad t_c = \tfrac{1}{2}t_a \end{aligned} \tag{5}$$

$$\begin{aligned} &\text{d)} \quad K^+(k)K^-(p) \to \pi^+(k')\pi^-(p') \\ &\quad t_d = -\tfrac{1}{6f^2}(s + t - 2u + m_K^2 + m_\pi^2) \end{aligned} \tag{6}$$

$$\begin{aligned} &\text{e)} \quad K^+(k)K^-(p) \to \pi^0(k')\pi^0(p') \\ &\quad t_e = -\tfrac{1}{12f^2}(2s - t - u + 2m_K^2 + 2m_\pi^2) \end{aligned} \tag{7}$$

$$\begin{aligned} &\text{f)} \quad K^0(k)\bar{K}^0(p) \to \pi^+(k')\pi^-(p') \\ &\quad t_f = -\tfrac{1}{6f^2}(s + u - 2t + m_K^2 + m_\pi^2) \end{aligned} \tag{8}$$

$$\begin{aligned} &\text{g)} \quad K^0(k)\bar{K}^0(p) \to \pi^0(k')\pi^0(p') \\ &\quad t_g = t_e \end{aligned} \tag{9}$$

$$\text{h)} \quad K^+(k)\bar{K}^-(p) \to \pi^0(k')\eta(p') \qquad t_h = -\frac{\sqrt{3}}{12f^2}(2s - t - u + \frac{2}{3}m_\pi^2 - \frac{2}{3}m_K^2) \tag{10}$$

$$\text{i)} \quad K^0(k)\bar{K}^0(p) \to \pi^0(k')\eta(p') \qquad t_i = -t_h \tag{11}$$

$$\text{j)} \quad \pi^0(k)\eta(p) \to \pi^0(k')\eta(p') \qquad t_j = -\frac{m_\pi^2}{3f^2} \tag{12}$$

$$\text{k)} \quad \pi^0(k)\pi^0(p) \to \pi^0(k')\pi^0(p') \qquad t_k = -\frac{m_\pi^2}{f^2} \tag{13}$$

$$\text{l)} \quad \pi^+(k)\pi^-(p) \to \pi^0(k')\pi^0(p') \qquad t_j = -\frac{1}{3f^2}(2s - u - t + m_\pi^2) \tag{14}$$

$$\text{m)} \quad \pi^+(k)\pi^-(p) \to \pi^+(k')\pi^-(p') \qquad t_m = -\frac{1}{3f^2}(s + t - 2u + 2m_\pi^2) \tag{15}$$

where $s = (k+p)^2, t = (k-k')^2, u = (k-p')^2$

In order to obtain the S-wave amplitudes in the different isospin channels we construct the isospin eigenstates projecting over and S-wave satate . We have

$$T = 0$$

$$|K\bar{K}> = -\frac{1}{\sqrt{2}}\sum_{\vec{q}} f(q)|K^+(\vec{q})K^-(-\vec{q}) + K^0(\vec{q})\bar{K}^0(-\vec{q})> \tag{16}$$

$$|\pi\pi> = -\frac{1}{\sqrt{6}}\sum_{\vec{q}} f(q)|\pi^+(\vec{q})\pi^-(-\vec{q}) + \pi^-(\vec{q})\pi^+(-\vec{q}) + \pi^0(\vec{q})\pi^0(-\vec{q})>$$

$$T = 1$$

$$|K\bar{K}> = -\frac{1}{\sqrt{2}}\sum_{\vec{q}} f(q)|K^+(\vec{q})K^-(-\vec{q}) - K^0(\vec{q})\bar{K}^0(-\vec{q})> \tag{17}$$

$$|\pi\eta> = \sum_{\vec{q}} f(q)|\pi^0(\vec{q})\eta(-\vec{q})>$$

where $\vec{q}$ is the momentum of the particles in the CM of the pair and $q = |\vec{q}|$. We have used the convention that $|\pi^+> = -|1,1>$ and $|K^+> = -|\frac{1}{2},\frac{1}{2}>$ isospin states. Note that for symmetry reasons there is no $\pi\pi$ S-wave, $T = 1$ state. The function $f(q)$ is normalized such that $\sum_{\vec{q}} f^2(q) = 1$ and we take it as infinitely peaked around a certain value q. Note also the apparent extra normalization factor $1/\sqrt{2}$ in the $|\pi\pi, T = 0>$ state which is a consequence of its symmetry (particles and antiparticles go into the same multiplet of isospin). By taking into account eqs. (17),(18) and the amplitudes in eqs. (3) to (15) we can write now:

$$
\begin{aligned}
&T=0\\
&V_{11}=-<K\bar{K}|\mathcal{L}_2|K\bar{K}>=-\tfrac{1}{4f^2}(3s+4m_K^2-\textstyle\sum_i p_i^2)\\
&V_{21}=-<\pi\pi|\mathcal{L}_2|K\bar{K}>=-\tfrac{1}{3\sqrt{12}f^2}(\tfrac{9}{2}s+3m_K^2+3m_\pi^2-\tfrac{3}{2}\textstyle\sum_i p_i^2)\\
&V_{22}=-<\pi\pi|\mathcal{L}_2|\pi\pi>=-\tfrac{1}{9f^2}(9s+\tfrac{15m_\pi^2}{2}-3\textstyle\sum_i p_i^2)
\end{aligned}
\tag{18}
$$

$$
\begin{aligned}
&T=1\\
&V_{11}=-<K\bar{K}|\mathcal{L}_2|K\bar{K}>=-\tfrac{1}{12f^2}(3s-\textstyle\sum_i p_i^2+4m_K^2)\\
&V_{21}=-<\pi^0\eta|\mathcal{L}_2|K\bar{K}>=\tfrac{\sqrt{3/2}}{12f^2}(6s-2\textstyle\sum_i p_i^2+\tfrac{4}{3}m_\pi^2-\tfrac{4}{3}m_K^2)\\
&V_{22}=-<\pi^0\eta|\mathcal{L}_2|\pi^0\eta>=-\tfrac{1}{3f^2}m_\pi^2
\end{aligned}
\tag{19}
$$

where $p_1=k\ ,p_2=p\ ,p_3=k'\ ,p_4=p'$ and the sum over momenta squared runs from 1 to 4. For on shell amplitudes $p_i^2=m_i^2$.

3 $L=0,T=0,1$ strong amplitudes in the coupled channel approach

It is easy to see that if one iterates the lowest order amplitudes calculated before, introducing loops, and one evaluates the finite contributions to the imaginary part of the amplitudes, the higher order contributions at energies around 1 GeV or below are even larger than those of the lowest order. Furthermore, we have the resonances f_0 ,a_0 in the $L=0$ channel around the $K\bar{K}$ threshold which should appear as singularities in the t matrix. It is then clear that the standard χPT expansion, keeping a few orders, neither will converge nor give this analytical structure. This difficulty is expectable since one is making an expansion in powers of p^2/Λ_χ^2, and we go up to energies $\sqrt{s}=1.2\ GeV$. In order to overcome these problems we assume that the lowest order Hamiltonian provides us with the potential that we iterate in the Lippmann Schwinger equation with two coupled channels, using relativistic meson propagators in the intermediate states. This idea follows identical assumptions made in refs. [34, 35] in the meson-baryon sector. Our channels are labelled 1 for the $K\bar{K}$ and 2 for the $\pi\pi$ states in $T=0$ and 1 for $K\bar{K}$, 2 for $\pi\eta$ in $T=1$. The coupled channel equations then become

$$
\begin{aligned}
t_{11}&=V_{11}+V_{11}G_{11}t_{11}+V_{12}G_{22}t_{21}\\
t_{21}&=V_{21}+V_{21}G_{11}t_{11}+V_{22}G_{22}t_{21}\\
t_{22}&=V_{22}+V_{21}G_{11}t_{12}+V_{22}G_{22}t_{22}
\end{aligned}
\tag{20}
$$

$$G_{ii} = i\frac{1}{q^2 - m_{1i}^2 + i\epsilon} \ \frac{1}{(P-q)^2 - m_{2i}^2 + i\epsilon} \tag{21}$$

where P is the total fourmomentum of the meson-meson systems and q the fourmomentum of one intermediate meson. The terms VGT in eq. (20) actually mean

$$VGT = \int \frac{d^4q}{(2\pi)^4} V(k,p;q) G(P,q) t(q;k',p') \tag{22}$$

Note that as G_{ii} has no angular dependence and V_{ij} is purely S-wave then t_{ij} is S-wave.

The diagrammatic meaning of eqs. (20) is shown in fig. 1.

The loop integral in eq. (22) is divergent. In χPT these divergences are cancelled by counterterms of chiral Lagrangians at higher order and some finite contribution remains from the loops and the counterterms. In our approach we take a cut off q_{max} for the maximum value of the modulus of the momentum q. We vary this parameter in order to fix some property of the data (for example the position of the maximum of an experimental cross sections) and after this is done there is no freedom in our model. On grounds of chiral symmetry computations we should expect this cut off to be around $1\,GeV$ [36].

By fixing the cut off one generates the counterterms in our scheme. It is also relevant to see that since our scheme produces the σ , f_0 , a_0 resonances, our work makes connection with the work of ref. [37] where the finite parts of the counterterms are generated from the exchange of resonances.

It is also clear that our non perturbative method does not generate all the terms which appear in the standard χPT expansion. For instance loops in the t-channel are not accounted for. But the fact that the scheme proves so successful, as we shall see, indicates that one is summing the relevant infinite series needed to produce the structure of the t matrix. One can expect this because the singularities associated to these t-channel terms are far away from the physical region, contrary to what happens with the s-channel terms summed up in the Lippmann Schwinger equation, which lead to the pole structure of the amplitudes, essential to reproduce the physical scattering amplitudes.

In principle one would have to solve the integrals in eqs. (20) by taking V and t off shell. However, this is not the case, as we show below, at least when dealing with S-wave, and we only need the on shell information. The argument goes as follows: As we can see from eqs. (18),(19), the on shell amplitudes are obtained by taking $p_i^2 = m_i^2$ and then we can write the off shell amplitudes as

$$V = V_{on} + \beta \sum_i (p_i^2 - m_i^2)$$

In order to illustrate the procedure let us simplify to one loop and one channel (the procedure is easily generalized to two channels). Hence we have

$$V^2 = V_{on}^2 + 2\beta V_{on} \sum_i (p_i^2 - m_i^2) + \beta^2 \sum_{ij} (p_i^2 - m_i^2)(p_j^2 - m_j^2) \tag{23}$$

When performing the q^0 integration in the loop we have two poles, one for $q^0 = w_1(q)$ and the other one for $q^0 = P^0 + w_2(q)$, where the indices 1 and 2 indicate the two mesons inside the loop. Let us take the contribution from the first pole (the procedure follows analogously for the second pole). From the second term in eq. (23) we get the contribution

$$\frac{2\beta V_{on}}{(2\pi)^3}\int \frac{d^3q}{2w_1(q)}\frac{(P^0-w_1)^2-w_2^2}{(P^0-w_1)^2-w_2^2} = \frac{\beta V_{on}}{(2\pi)^3}\int dw_1 q \tag{24}$$

which for large Λ compared to the masses goes as $V_{on}\Lambda^2$ and has the same structure in the dynamical variables as the tree diagram. The third term in eq. (23) gives rise to the integral

$$\frac{\beta^2}{(2\pi)^3}\int \frac{d^3q}{2w_1(q)}[(P^0-w_1)^2-w_2^2] = \frac{\beta^2}{(2\pi)^3}\int \frac{d^3q}{2w_1(q)}[P^{02}-2w_1P^0+(m_1^2-m_2^2)] \tag{25}$$

coming from the first pole ($q^0 = w_1(q)$) and

$$\frac{\beta^2}{(2\pi)^3}\int \frac{d^3q}{2w_2(q)}[P^{02}+2w_2P^0+(m_2^2-m_1^2)]$$

coming from the second pole ($q^0 = P^0 + w_2(q)$). As we can see, the terms linear in P^0 cancel exactly, respecting the chiral structure which does not allow linear terms in P^0.

The term proportional to $P^{02}+m_1^2-m_2^2$ in (25) leads again to a structure of the type $[P^{02}+(m_1^2-m_2^2)]\Lambda^2$ and similarly happens with the quadratic contribution form the second pole which leads to $[P^{02}+(m_2^2-m_1^2)]\Lambda^2$. These terms, together the $V_{on}\Lambda^2$ which we obtained before, combine with the tree level contribution, giving rise to an amplitude with the same structure as the tree level one but with renormalized parameters f and masses. However, since we are taking physical values for $f(f = f_\pi = 93\,MeV)$ and the masses in the potential, these terms should be omitted. One can proceed like that to higher orders with the same conclusions.

Since we are taking V and t on shells they factorize outside the q integral. Thus the term VGT of eq. (22), after the q^0 integration is performed by choosing the contour in the lower half of the complex plane, is given by

$$\begin{aligned} &V_{ij}G_{jj}t_{jk} = V_{ij}(s)t_{jk}(s)G_{jj}(s) \\ &G_{jj}(s) = \int_0^{q_{max}} \frac{q^2dq}{(2\pi)^2}\frac{\omega_1+\omega_2}{\omega_1\omega_2[P^{02}-(\omega_1+\omega_2)^2+i\epsilon]} \end{aligned} \tag{26}$$

where $\omega_i = (\vec{q}^{\,2}+m_i^2)^{1/2}$ and $P^{02} = s$ and the subindex i stands for the two intermediate mesons of the j channel.

Thus the coupled channel Lippmann Schwinger equations get reduced to a set of algebraic equations:

$$At = V \tag{27}$$

where

$$t = \begin{pmatrix} t_{11} \\ t_{21} \\ t_{22} \end{pmatrix} \qquad V = \begin{pmatrix} V_{11} \\ V_{21} \\ V_{22} \end{pmatrix}$$
$$A = \begin{pmatrix} 1 - V_{11}t_{11} & -V_{12}G_{22} & 0 \\ -V_{21}G_{11} & 1 - V_{22}G_{22} & 0 \\ 0 & -V_{21}G_{11} & 1 - V_{22}G_{22} \end{pmatrix} \tag{28}$$

Introducing the notations

$$\begin{aligned} \Delta_\pi &= 1 - V_{22}G_{22} \\ \Delta_K &= 1 - V_{11}G_{11} \\ \Delta_c &= \Delta_K\Delta_\pi - V_{12}^2 G_{11}G_{22} \\ \Delta &= detA = \Delta_\pi\Delta_c \end{aligned} \tag{29}$$

and inverting the matrix A we obtain the following equations

$$\begin{aligned} t_{11} &= \tfrac{1}{\Delta_c}(\Delta_\pi V_{11} + V_{12}^2 G_{22}) \\ t_{21} &= \tfrac{1}{\Delta_c}(V_{21}G_{11}V_{11} + \Delta_k V_{21}) \\ t_{22} &= \tfrac{V_{22}}{\Delta_\pi} + \tfrac{V_{12}^2 G_{11}}{\Delta_\pi\Delta_c} \end{aligned} \tag{30}$$

where we have used the fact that $V_{12} = V_{21}$ and $t_{12} = t_{21}$ by time reversal invariance.

The physical amplitudes as a function of s (real variable) are given by the expressions in eqs. (30). However, in order to explore the position of the poles of the scattering amplitudes one must take into account the analytical structure of these amplitudes in the different Riemann sheets. These sheets appear because of the cuts related to the opening of thresholds in $G_{jj}(s)$ (see fig. 2). By denoting p_1 for the CM trimomentum of the K in the $K\bar{K}$ system and p_2 for the π in the $\pi\pi, T = 0$ system or the π in the $\pi\eta, T = 1$ systems

$$p_i = \frac{[s - (m_{1i} + m_{2i})^2]^{1/2}[s - (m_{1i} - m_{2i})^2]^{1/2}}{2\sqrt{s}} \tag{31}$$

The sheets which we consider are

$$\begin{aligned} &\text{Sheet I}: && Im\, p_1 > 0,\ Im\, p_2 > 0 \\ &\text{Sheet II}: && Im\, p_1 > 0,\ Im\, p_2 < 0 \\ &\text{Sheet III}: && Im\, p_1 < 0,\ Im\, p_2 < 0 \\ &\text{Sheet IV}: && Im\, p_1 < 0,\ Im\, p_2 > 0 \end{aligned} \tag{32}$$

In order to make an analytical extrapolation to the II, III and IV Riemann sheets we have to cross the cuts $G_{ii}(P^0)$. In order to do this we make use of the continuity property (for real $P^0 > m_{1i} + m_{2i}$)

$$G_{ii}^{(b)}(P^0 + i\epsilon) = G_{ii}^{(a)}(P^0 - i\epsilon) \tag{33}$$

where the index (b) indicates that we are in the second Riemann sheet of G_{ii} while the index (a) indicates the first Riemann sheet. Then

$$\begin{aligned} G_{ii}^{(b)}(P^0 + i\epsilon) &= G_{ii}^{(a)}(P^0 - i\epsilon) = G_{ii}^{(a)}(P^0 + i\epsilon) - 2iImG_{ii}^{(a)}(P^0 + i\epsilon) = \\ &= G_{ii}^{(a)}(P^0 + i\epsilon) + \tfrac{i}{4\pi}\tfrac{[P^{02}-(m_{1i}+m_{2i})^2]^{1/2}[P^{02}-(m_{1i}-m_{2i})^2]^{1/2}}{2P^{02}} \end{aligned} \tag{34}$$

We use the first and last terms of these equations to extrapolate $G_{ii}^{(b)}$ in the complex P^0 plane (the square root is taken such that Im $\surd > 0$). Thus the sheet I is obtained with $G_{11}^{(a)}, G_{22}^{(a)}$; the sheet II with $G_{22}^{(b)}, G_{11}^{(a)}$; the sheet III with $G_{22}^{(b)}, G_{11}^{(b)}$ and the sheet IV with $G_{22}^{(a)}, G_{11}^{(b)}$.

4 Results

4.1 Phase shifts and Inelasticities:

It is interesting to stress that we have only one free parameter at our disposal, which for chiral symmetry reasons should be of the the order of the 1 GeV. We have taken as our ultimate choice $q_{max} = 1.1\ GeV$ which gives a good agreement with experiment in all channels for phase shifts and decay widths of the resonances. In order to obtain the phase shifts and inelasticities we use the two-channel S matrix [15]

$$S = \begin{bmatrix} \eta e^{2i\delta_1} & i(1-\eta^2)^{1/2}\, e^{i(\delta_1+\delta_2)} \\ i(1-\eta^2)^{1/2} e^{i(\delta_1+\delta_2)} & \eta e^{2i\delta_2} \end{bmatrix} \tag{35}$$

where δ_1, δ_2 are the phase shifts for the 1 and 2 channels ($K\bar{K}, \pi\pi$ in $T = 0$ and $K\bar{K}, \pi\eta$ in $T = 1$ respectively) and η is the inelasticity. The elements in the S matrix are related to our amplitudes via:

$$\begin{aligned} t_{11} &= -\tfrac{8\pi\sqrt{s}}{2ip_1}(S_{11} - 1) \\ t_{22} &= -\tfrac{8\pi\sqrt{s}}{2ip_2}(S_{22} - 1) \\ t_{12} = t_{21} &= -\tfrac{8\pi\sqrt{s}}{2i\sqrt{p_1 p_2}}(S_{12} - 1) \end{aligned} \tag{36}$$

It is interesting to recall that the first two equations allow us to determine δ_1, δ_2 and η while the third equation allows us to determine δ_2 and η. We obtain the same results with both methods, which is a check of consistency of the exact unitarity implemented in our scheme. In fig. 3 we show the results for the $\pi\pi$ phase shifts

($\delta^0_{0\pi\pi}$) in $L=0,\ T=0$. We show in the figure the results for two values of the cut off energy $\Lambda = 1.1$ and $1.2\ GeV$ ($\Lambda = (q^2_{max} + m^2_K)^{1/2}$)

We can see that the agreement with the experiment [1,38–45] is rather good up to values of $\sqrt{s} = 1.2\ GeV$. From there on discrepancies with experiment start to appear, but this should be expected because of the opening of the $\eta\eta$ channel, the increasing importance of the 4π channel and the possible influence of higher resonances which cannot be considered as meson-meson states. We can see that the position of the f_0 resonance is well reproduced. On the other hand the results are moderately dependent on the cut off. At low energies, $\sqrt{s} < 500\,MeV$ we can see that our results are rather independent of the cut off and agree with the data of ref. [45]. Another feature worth mentioning is a bump in our results around $\sqrt{s} = 500 - 800\,MeV$ and in some experimental analyses, which in our case is originated, as we shall see, by the presence of the σ pole.

In fig. 4 we show our results for the phase shift of $K\bar{K} \to \pi\pi$, $(\delta_1 + \delta_2)$ obtained through eqs.(35), compared to the experimental results of ref. [46, 47]. The agreement with the data is also good. We have also calculated the results with $\Lambda = 1.1\,GeV$ and $1.2\ GeV$ and although both are compatible with the data, we can see a better agreement with the data with smaller error for $\Lambda = 1.2\ GeV$. The agreement with these two sets of data guarantees agreement with the $K\bar{K}$ phase shifts, which are obtained from these data by using the two channel unitarity of eq. (35).

In fig. 5 we show the results for the inelasticity using $\Lambda = 1.2\,GeV$. There is an obvious discrepancy between different data [45–48]. Nevertheless, we observe a good agreement of our results with the data of ref. [46] in consistency with the agreement found before for the phase shifts $\delta^0_{0\,KK,\pi\pi}$ coming from the same analysis [46]. It should be noted here that in ref. [16] one obtains agreement with the upper set of data from ref. [48].

For the $T=1$ channel the data are scarce and different analyses on the same magnitude, which would show independence on assumptions made, are lacking. We can compare our results with data for $\pi\eta$ invariant mass distributions coming from the reaction $K^- p \to \Sigma^+(1385)\pi^-\eta$ [49]. Similarly we can analyse $K^- p \to \Sigma^+(1385)K^-K^0$. Following ref. [50] we write

$$\frac{d\sigma_\alpha}{dm_\alpha} = C|t_\alpha|^2 q_\alpha \tag{37}$$

where m_α is the invariant mass of the $\pi^-\eta(K^-K^0)$ system, q_α is the $\pi^-(K^-)$ momentum in the $\pi^-\eta(K^-K^0)$ CM frame, t_α is the scattering amplitude of the $\pi^-\eta(K^-K^0)$ system and C a normalization constant.

In fig. 6 we can see the $\pi^-\eta$ invariant mass distribution and our results with two different normalization constants. In fig. 7 we show the same results for the K^-K^0 invariant mass with the corresponding normalization constants.

The peak in the $\pi^-\eta$ mass distribution is due to the dominance of the a_0 resonance. We can see that we also produce the peak at the same place as the experiment and reproduce qualitatively the data. The agreement found with the K^-K^0 mass distribution is also qualitatively good.

4.2 Poles and widths

.

In order to determine the "true" mass and width of the σ, f_0 and a_0 resonances one has to look for the position of the poles in the physical amplitudes in the complex P^0 plane. In the $T = 0$ channel we find a pole in the II sheet of the complex plane which corresponds to the f_0 resonance at $P^0_{f_0} = (981.4 + i\,22.4)\ MeV$, corresponding to a mass $M_{f_0} = 981.4\ MeV$ and a width $\Gamma_{f_0} = 44.8\ MeV$. This singularity results in a peak in the physical amplitudes $\pi\pi \to K\bar{K}$ as one can see in fig. 8.

We find another pole in the $T = 0$ channel corresponding to the σ. Actually we find two poles corresponding to zeros of Δ_π and Δ_c in eq. (29) which are very close. The zero of Δ_π appears at $P^0_\sigma = (468.5 + i\,193.6)\,MeV$ while the zero of Δ_c appears at $P^0_\sigma = (469.5 + i\,178.6)\ MeV$. The fact that the two poles are so close and the associated width so large makes that in practice one only sees one bump in the cross section. In any case the second term of t_{22} in eq. (30) is very small in the σ region in the physical sheet (sheet I). It should be noted that the σ pole in Δ_c also affects the t_{11}, t_{21} amplitudes, but this has scarce practical consequences since this appears in the unphysical region below threshold and the physical region near threshold is dominated by the f_0 pole.

The σ that we find is rather broad with $\Gamma_\sigma \simeq 400\ MeV$. We should also note that since it comes essentially from the first term of t_{22} in eq. (30), it is practically tied exclusively to the pion sector, with practically no influence from the $K\bar{K}$ sector. Hence, if we eliminate the $K\bar{K}$ channel from our coupled equations the σ pole survives.

In the case of the f_0 we have also observed that it is dominated by the $K\bar{K}$ channel, in the sense that if we eliminate the $\pi\pi$ channel (setting $V_{12} = 0$) the f_0 pole appears also, now at $P^0_{f_0} = (973.4 + i0)\,MeV$. The zero width is obvious in this case since there is no decay into $\pi\pi$, nor possible $K\bar{K}$ decay because one is below threshold. In the case when the $\pi\pi$ decay channel is open, the $K\bar{K}$ channel also opens because the finite f_0 width gives phase space for the decay into $K\bar{K}$ (we will come back to this).

In the $T = 1$ channel we find a pole in the II sheet corresponding to the a_0 at a position $P^0_{a_0} = (973.2 + i\,85.0)\ MeV$. This corresponds to a width of $\Gamma_{a_0} = 170\ MeV$. This pole is much tied to the coupled channel. Indeed, if we eliminate the $\eta\pi$ channel (setting $V_{12} = 0$) the pole disappears.

In fig. 8 and 9 we show the results for the $|t_{12}|^2$ around the f_0 and a_0 regions respectively. We see there two peaks corresponding to the resonance excitation around $\sqrt{s} = 987\ MeV$ for the f_0 and $982\ MeV$ for the a_0. The naive widths that one observes there are around $20\ MeV$ and $60\ MeV$ respectively. The position of the peaks and the "widths" do not correspond exactly to the numbers of the pole position. This is a well know fact of resonances. However, in the present case there is one extra feature, which is mostly responsible for the shrinking of the width and change of position of the maximum. This was discussed in ref. [50] for the specific case of the a_0, but the arguments hold also for the f_0. This feature is a cusp effect, due to the strong coupling of the resonances to the $K\bar{K}$ channel which appears around the pole position. This makes the $K\bar{K}$ decay width to increase very fast as the energy increases, reducing the amplitudes accordingly and producing a shift of the peak

position. Large widths for the a_0 around 200 MeV have also been claimed in former studies [16].

5 Strong partial decay widths

The particular structure of the amplitudes t_{11}, t_{21}, t_{22} of eq.(30) makes that the t_{11} and t_{12} amplitudes in $T = 0$ have a peak around the f_0 pole, while the $\pi\pi$ amplitude combines the f_0 pole with a background coming from the terms that give rise to the σ pole and one has actually a minimum around that region. In the case of $T = 1$ all these amplitudes peak around the a_0 pole. In view of this, we take the t_{11} and t_{12} amplitudes in both cases and parametrize them around the resonance region in terms of a Breit Wigner expression with energy dependent widths.

$$\begin{aligned} t_{11} &= \frac{1}{2M_R}\frac{g_{R1}^2(s)}{\sqrt{s}-M_R+i\frac{\Gamma_R(s)}{2}} \\ t_{21} &= \frac{1}{2M_R}\frac{g_{R1}(s)g_{R2}(s)}{\sqrt{s}-M_R+i\frac{\Gamma_R(s)}{2}} \end{aligned} \tag{38}$$

We shall not need the explicit values of $g_{Ri}(s)$ and $\Gamma_R(s)$ since we can compute our final expressions in terms of $Im\, t_{j1}$ as shown below.

In order to evaluate the partial decays widths we take into account the finite width of the resonance and substitute in the standard formula for the decay width

$$2\pi\delta(M_\alpha - \omega_1 - \omega_2) \to 2Im\ \frac{1}{M_R - \omega_1 - \omega_2 - i\frac{\Gamma_R}{2}} \tag{39}$$

in view of which the partial decay widths are give by

$$\Gamma_{R,\alpha} = \frac{1}{16\pi^2}\int_{m_1+m_2}^{\infty} dW \frac{q}{W^2}\,|g_{R\alpha}(W)|^2 \frac{\Gamma_R}{(M_R - W)^2 + (\frac{\Gamma_R(W)}{2})^2} \tag{40}$$

However in practical terms we write eq. (40) in terms of the amplitudes of eq. (36) directly and we find

$$\begin{aligned} \Gamma_{R,1} &= -\tfrac{1}{16\pi^2}\textstyle\int_{m_1+m_2}^{\infty} dW\ \frac{q}{W^2} 4M_R Im t_{11} \\ \Gamma_{R,2} &= -\tfrac{1}{16\pi^2}\textstyle\int_{m_1'+m_2'}^{\infty} dW\ \frac{q}{W^2} 4M_R \frac{(Im t_{21})^2}{Im t_{11}} \end{aligned} \tag{41}$$

We integrate in W around two widths up and down the peak (if allowed by the lower limit) where we find that $\Gamma_{R,1}+\Gamma_{R,2} = \Gamma_{tot}$, where Γ_{tot} is the width corresponding to the pole of the amplitude evaluated before.

In table I we give the results of the partial widths and the mass of the f_0. Both the pole position and the peak of the t_{21} amplitude are in agreement with the results of the particle data group [51]. As with respect to the width, Γ_{tot} is also compatible with most of the present data as can be seen in ref. [51]. The ratio $\Gamma_{\pi\pi}/(\Gamma_{\pi\pi} + \Gamma_{K\bar{K}})$ is also in good agreement with the different measurements, as can be seen in table I. Since $K\bar{K}$ branching ratio is obtained by subtraction from unity of the $\pi\pi$ branching ratio, our results are also compatible with those quoted in the particle data book.

In table II we give the results for the a_0. The mass quoted in the PDB [51] is in agreement with our results for the peak position of the t_{21} amplitude. Although the position of the pole of the amplitude appears at a different energy. This difference between the pole position and the peak of physical amplitudes is well known in general [62]. The width of the resonance is $\Gamma_{tot} = 170\ MeV$, apparently larger than many of the experimental numbers in [51]. However, we already quoted how the cusp effect can convert this large width into experimental narrower amplitudes [50] and this was indeed the case in our results as shown in fig. 9. We also quoted our qualitative agreement with other theoretical results [16] which have $\Gamma_{a_0} = 202\ MeV$. Another interesting piece of data is the fraction of $K\bar{K}$ decay into $\eta\pi$. This fraction is practically unity in our approach and compatible with the most recent measurement of ref. [58]. We should note that the fact that the fraction of $K\bar{K}$ to $\eta\pi$ decay is large is due to the fact that the a_0 width is large, since for narrow resonances there would be little phase space for $K\bar{K}$ decay.

As we see, we can claim a global good agreement with experiment for masses and partial strong decay widths.

6 Decay of the resonances into $\gamma\gamma$

In order to determine the decay width of the a_0 and f_0 resonances into the $\gamma\gamma$ channel we proceed in an analogous way as done for the strong decays. In the first place we obtain the $K\bar{K} \to \gamma\gamma$ amplitude using the coupled channel approach discussed above, and second we obtain the effective coupling of the resonances to the $\gamma\gamma$ channel in order to obtain the partial decay width via eq. (41). The Lippmann Schwinger equation for the amplitude $K\bar{K} \to \gamma\gamma$ would now be written as

$$t_{\gamma 1} = V_{\gamma 1} + V_{\gamma 1} G_{11} t_{11} + V_{\gamma 2} G_{22} t_{21} \tag{42}$$

where now $V_{\gamma 1}, V_{\gamma 2}$ are the potentials obtained from the chiral Lagrangian at lowest order with external electromagnetic currents [63, 64]:

$$\begin{aligned} V_{\gamma\gamma K^+K^-} &= -2ie^2 \left\{ \epsilon_\mu^1 \epsilon^{\mu(2)} - \tfrac{k_+\cdot\epsilon_1\, k_-\cdot\epsilon_2}{k_+\cdot k_1} - \tfrac{k_+\cdot\epsilon_2\, k_-\cdot\epsilon_1}{k_+\cdot k_2} \right\} \\ V_{\gamma\gamma\pi^0\eta} &= 0 \\ V_{\gamma\gamma\pi^+\pi^-} &= -2ie^2 \left\{ \epsilon_\mu^{(1)} \epsilon^{\mu(2)} - \tfrac{p_+\cdot\epsilon_1\, p_-\cdot\epsilon_2}{p_+\cdot k_1} - \tfrac{p_+\cdot\epsilon_2\, p_-\cdot\epsilon_1}{p_+\cdot k_2} \right\} \end{aligned} \tag{43}$$

In eq. (43), following the nomenclature of ref. [64] we have k_1, k_2 the photon momenta, ϵ_1, ϵ_2 their polarization vectors, and k_+, k_-, p_+, p_- the momenta of the K^+, K^-, π^+, π^- respectively. We also take the same gauge as in ref. [64] in order to perform the calculations, $\epsilon_1 \cdot k_1 = \epsilon_1 \cdot k_2 = \epsilon_2 \cdot k_1 = \epsilon_2 \cdot k_2 = 0$. From eqs. (43) and the isospin states of eqs. (16),(17) we obtain the S-wave $V_{\gamma i}$ potentials. We factorize the on shell t matrices and $V_{\gamma 1}$ outside the integrals in $V_{\gamma 1} G_{ii} T_{11}$ in eq. (41), as we did in the strong amplitudes, and we evaluate the integrals of G_{ii} cutting the integral over momentum at the same value of q_{max}. Since the scattering amplitudes t_{i1} are evaluated before, the evaluation of $t_{\gamma 1}$ of eq. (42) is straightforward. Since both t_{11}

and t_{21} become singular at the f_0, a_0 poles, the $t_{\gamma 1}$ amplitude also has a singularity there in the $T=0$, $T=1$ channels respectively.

It is interesting to recall than the standard χPT expansion acounts for some terms not accounted for here [64]. Once again, if these terms were added to our amplitude they could not change the resonant part of the $t_{\gamma 1}$ amplitude of eq.(42) given by t_{11} and t_{21} and which is observed experimentally for $\gamma\gamma \to \pi^+\pi^-, \pi^0\pi^0, \pi^0\eta$ [26].

By following similar steps as for the strong decay we can write

$$\Gamma_{R,\gamma\gamma} = -\frac{1}{2}\frac{1}{16\pi^2}\int_{m_1+m_2}^{\infty} dW \frac{q}{W^2} 4M_R \frac{(Imt_{1\gamma})^2}{Imt_{11}} \tag{44}$$

where m_1, m_2 refer now to $2m_\pi, (m_\pi + m_\eta)$ for $T=0, (T=1)$ since below this value there is no imaginary part of $ImT_{1\gamma}$. The factor $1/2$ in eq. (44) is due to identity of the two final photons. As we did before, we integrate over W in an interval of 2Γ above M_R and 2Γ below, if allowed by phase space.

The results for the widths are shown in tables I and II for the f_0 and a_0 respectively. We see a very good agreement with the PDB averages which are compatible with many of the different results of the analyses quoted in those tables. In any case the situation is still problematic, as it is reflected in table I in the dispersion of the quoted results of the analyses. In fact in this sector,$T=0$ and $L=0$, it is not understood why a broad scalar structure above $1\,GeV$ is observed for $\gamma\gamma \to \pi^+\pi^-$, following ref. [4], and it is not seen in $\gamma\gamma \to \pi^0\pi^0$. On the other hand for the $T=1, L=0$ channel the problems come from the way one isolates the background around the well observed $a_0(980)$ and $a_2(1320)$ resonances in the $\gamma\gamma \to \pi^0\eta$ reaction, with its influence on the coupling to two photons of the former resonances. All these problems are properly reviewed in [26].

7 Conclusions

We have used a non perturbative approach to deal with the meson meson interaction in the scalar sector at energies below $\sqrt{s} \simeq 1.2\ GeV$, exploiting chiral symmetry and unitarity in the coupled channels. The Lippmann Schwinger equation with coupled channels, using relativistic meson propagators, and the lowest order chiral Lagrangians, providing the meson-meson potential, are the two ingredients of the theory. One cut off in momentum, expected to be of the order of $1\ GeV$, is also used in order to cut the loop integrals and it is fine tuned in order to obtain essentially the position of the poles. This is the only parameter of the theory. The best fit to all the data is found with $q_{max} \simeq 1.1\ GeV$, or equivalently $\Lambda = 1.2\ GeV$, both for the $T=0$ and $T=1$ channels. We find poles for the f_0 and a_0 resonances, for $T=0$ and $T=1$ respectively, and also for the σ in the $T=0$ channel which appears as a broad resonance ($\Gamma = 400\,MeV$) at about $500\ MeV$ of energy.

We compute the $T=0$ phase shifts and inelasticities for $\pi\pi \to \pi\pi$, $\pi\pi \to K\bar{K}$ and $K\bar{K} \to K\bar{K}$ and they are in good agreement with experiment. In the case $T=1$ we look for mass distributions of $\pi^0\eta$ and $K\bar{K}$ which are also in agreement with poorer experimental data.

We also compute the partial decay widths of the $\pi\pi, K\bar{K}$ and $\pi^0\eta, K\bar{K}$ respectively and the results are in good agreement with experiment. We have also studied the partial decay mode of the resonances into $\gamma\gamma$. We show that the $K\bar{K} \to \gamma\gamma$ amplitude (as well as other ones) contains the f_0 and a_0 poles in the $T = 0$ and $T = 1$ channels respectively and we have evaluated the decay width of the a_0 and f_0 resonances into the $\gamma\gamma$ channel. The results obtained are in good agreement with experiment.

The scheme used has proved to be very successful. The amount of data that one can reproduce using one only parameter is really impressive. We should recall that fits to some of the data studied here required a large number of parameters. On the other hand it is remarkable to see that this parameter is actually of the order of magnitude of what we could expect from former studies of chiral perturbation theory.

The teaching of the present results is that the constraints of chiral symmetry at low energies and the implementation of unitarity with the coupled channels, keeping also the real part of the loops, is the basic information which is contained in the meson-meson interaction in the scalar sector below $\sqrt{s} = 1.2\, GeV$.

On the other hand it is quite clear that the present scheme has allowed us to make progress within the lines of chiral dynamics, introducing a non perturbative method which allow us to go to higher energies than in χPT and at a lower price in the number of parameters. It becomes appealing to exploit these ideas in other processes related to the scalar sector or try to extend it to other sectors in order to test the potentiality of the method and its limits.

Acknowledgements.

We would like to acknowledge fruitful discussions with our colleagues, A. Pich, J. Prades, J. Nieves and W. Weise. One of us J.A. O. would like to acknowledge financial help from the Generalitat Valenciana.

Table I: f_0 Mass and partial widths ($\Lambda = 1.2\,GeV$)

f_0	our results	experiment
Mass Pole position $[MeV]$	981.4	980 ± 10 [51]
Mass Peak of the t_{21} amplitude $[MeV]$	987	980 ± 10 [51]
Γ_{tot} [MeV]	44.8	40 - 100 [51]
$\frac{\Gamma_{\pi\pi}}{\Gamma_{\pi\pi}+\Gamma_{K\bar{K}}}$	0.75	0.67 ± 0.009 [52] $0.81 \pm^{0.004}_{0.009}$ [53] 0.78 ± 0.003 [54] (av.) 0.781 ± 0.024 [51]
$\Gamma_{\gamma\gamma}$ (KeV)	0.54	0.63 ± 0.14 [4] $0.42 \pm 0.06 \pm 0.18$ [55] $0.29 \pm 0.07 \pm 0.12$ [56] $0.31 \pm 0.14 \pm 0.09$ [57] (av) 0.56 ± 0.11 [51]

Table 2: a_0 Mass and partial width ($\Lambda = 1.2\,GeV$)

a_0	our results	experiment
Mass Pole position $[MeV]$	937.2	983.5 ± 0.9 [51]
Mass Peak of the t_{21} amplitude $[MeV]$	982	983 ± 0.9 [51]
Γ_{tot} [MeV]	170 (*)	50 - 100 [51]
$\frac{\Gamma_{K\bar{K}}}{\Gamma_{\eta\pi}}$	1.07	1.16 ± 0.18 [58] 0.7 ± 0.3 [59] 0.25 ± 0.008 [60]
$\frac{\Gamma_{\gamma\gamma}\cdot\Gamma_{\eta\pi}}{\Gamma_{tot}}$ $[KeV]$	0.22	$0.28 \pm 0.04 \pm 0.01$ [55] $0.19 \pm 0.07 \pm^{0.07}_{0.1}$ [61] av. $0.24 \pm^{0.007}_{0.008}$ [51]

(*) See discussion in the text about the narrower physical amplitudes because of the cusp effect.

FIGURES

Fig.1. Diagrammatic series for eqs. (20) for t^0_{11} with $T = 0$

Fig.2. Sheets in the complex energy plane. The unitarity cuts are indicated by thick lines.

Fig.3. $\delta^0_{0\pi\pi}$ phase shifts for $\pi\pi \to \pi\pi$ in $T = 0$ and $L = 0$ compared with different analyses indicated between brackets.

Fig.4. $\delta^0_{0K\bar{K}\pi\pi}$ phase shifts for $K\bar{K} \to \pi\pi$ in T=0 and L=0 compared with different analyses indicated between brackets.

Fig.5. $\frac{1-\eta^2_{00}}{4}$ in $T = 0$ and $L = 0$ compared with different analyses indicated between brackets.

Fig.6. $\pi^-\eta$ mass distributions. The data are from the reaction $K^-p \to \Sigma^+(1385)\pi^-\eta$ [49].

Fig.7. K^-K^0 mass distributions. The data are from the reaction $K^-p \to \Sigma^+(1385)K^-K^0$ [49].

Fig.8. $|t^0_{12}|^2$, $T = 0$, around the mass of the $f_0(980)$.

Fig.9. $|t^1_{12}|^2$, $T = 1$, around the mass of the $a_0(980)$.

References

[1] S.D. Protopopescu, M. Alson-Garnjost, Phys. Rev. D7 (1973) 1279.

[2] R. Ammar et. al., Phys Rev. Lett. 21 (1968) 1832.

[3] D. Morgan, Phys.Lett. B51 (1974) 71.

[4] D. Morgan and M.R. Pennington, Z. Phys. C48 (1990) 623.

[5] M. R. Pennington, Nucl. Phys.B (Proc. Suppl.) 21 (1991) 37.

[6] D. Morgan and M. R. Pennington, Phys. Rev. D48 (1993) 1185.

[7] D. Morgan and M.R. Pennington, Phys. Rev. D48 (1993) 5422.

[8] N.A. Törnqvist, Z.Phys. C68 (1995) 647.

[9] N.A. Törnqvist and M. Roos, Phys. Rev. Lett. 76 (1996) 1575.

[10] A. Bramon and E. Massó, Phys. Lett. 93B (1980) 65.

[11] R.J. Jaffe, Phys. Rev. D15 (1977) 267.

[12] R.J. Jaffe, Phys. Rev. D15 (1977) 281.

[13] J. Weinstein and N. Isgur, Phys. Rev. Lett. 48 (1982) 659.

[14] J. Weinstein and N. Isgur, Phys. Rev. D27 (1983) 588.

[15] J. Weinstein and N. Isgur, Phys. Rev. D41 (1990) 2236.

[16] G. Janssen, B.C. Pearce, K. Holinde and J. Speth, Phys. Rev. D52 (1995) 2690.

[17] L. Burakovsky and L.P. Horwitz, Preprint, LA-UR-96 1809.

[18] K.L. Au, D.Morgan and M.R.Pennington, Phys. Rev. D35 (1987) 1633.

[19] J.M. Bordes, V. Gimenez and J.A. Peñarrocha , Phys. Lett. B223 (1989) 251.

[20] A.V. Anisovich, V.V. Anisovich, Yu.D. Prokoshkin and A.V. Sarantsev, hep-ph/9610453.

[21] B.S. Zou and D. V. Bugg, Phys. Rev. D48 (1993) R3948.

[22] D. Morgan and M.R. Pennington, Phys. Lett. B258 (1991) 444.

[23] D. Morgan, Nucl. Phys. A543 (1992) 632.

[24] A.M. Badalyan, J.I. Polikarpov and Yu. A. Simonov, Phys. Rep. 82 (1982) 31.

[25] D. Lose, J.W. Durso, K. Holinde and J. Speth, Nucl. Phys. A516 (1990) 513.

[26] M. Feindt and J. Harjes, Nucl. Phys. B (Proc. Suppl.) 21 (1991) 61.

[27] T. Barnes, Phys. Lett, B165 (1985) 434.

[28] L. Montanet, Nucl. Phys. B (Proc. Suppl.) 39B (1995) 281.

[29] J. Gasser and H. Leutwyler, Nucl. Phys. B250 (1985) 465.

[30] U.G. Meissner, Rep. Prog. Phys. 56 (1993) 903. V. Bernard, N. Kaiser and U.G. Meissner, Int. Jour. Mod. Phys. E4 (1995) 193.

[31] A. Pich, Rep. Prog. Phys. 58 (1995) 563.

[32] G. Ecker, Prog. Part. Nucl. Phys. 35 (1995) 1.

[33] N.N. Achason and G.N. Schestakov, Phys. Rev. D49 (1994) 5779 L.

[34] N. Kaiser, P.B. Siege, W. Weise, Phys. Lett. B362 (1995) 23.

[35] N. Kaiser, P.B. Siegel, W. Weise, Nucl. Phys. A594 (1995) 325.

[36] A. Manohar and Georgi, Nucl. Phys. B234 (1984) 189.

[37] G. Ecker, J. Gasser, A. Pich and E. de Rafael, Nucl. Phys. B321 (1989) 311.

[38] G. Gayer et al., Nucl. Phys. B75. (1974) 189.

[39] B. Hyabs et al, Nucl. Phys. B64 (1973) 134.

[40] P. Estrabooks et al. AIP Conf. Proc. 13 (1973) 37.

[41] G. Grayer et al., Proc. 3rd Philadelphia Conf. on experimental meson spectroscopy, Philadelphia 1972 (American Institute of Physics, New York, 1972) p.5.

[42] G. Grayer et al., AIP Conf. Proc. 13 (1973) 117.

[43] G. Grayer et al., Paper No.768 Contributed to the 16 th Int. Conf. on high-energy physiscs, Batavia, 1972.

[44] W. Männer, Contribution to the IV th International Conference on Experimental Meson Spectoscopy, Boston, Massachusetts, U.S.A, April 1974, and CERN preprint.

[45] C.D. Frogatt and J.L. Petersen, Nucl. Phys. B129 (1977) 89.

[46] D.Cohen, Phys. Rev. D22 (1980) 2595.

[47] A.D. Martin and E. N. Ozmuth, Nucl. Phys. B158 (1979) 520.

[48] S.J. Lindenbaum and R.S. Longacre, Phys.Lett. B274 (1992) 492

[49] Amsterdam-CERN-Nijmegen-Oxford Collaboration, Phys. Lett. 63 B (1976) 220.

[50] S.M. Flatté, Phys. Let. 63B (1976) 224.

[51] R.M. Barnett et al., Phys. Rev. D. 54 (1996).

[52] P.F.Lovere et al., Z. Phys. C6 (1980) 187.

[53] N.M.Cason et al., Phys. Rev Lett. 41 (1978) 271.

[54] W.Wetzel et al., Nucl. Phys. B115 (1976) 208.

[55] T.Oest et al., Z. Phys. C47 (1990) 343.

[56] J.Boyer et al., Phys. Rev. D42 (1990) 1350.

[57] H.Marsiske et al., Phys. Rev. D41 (1990) 3324.

[58] D.V.Bugg et al., Phys. Rev. D50 (1994) 4412.

[59] M.J.Corden et al., Nucl. Phys. B144 (1978) 253.

[60] C.Defoix et al., Nucl. Phys. B44 (1972) 125.

[61] D.Antreasyan et al., Phys. Rev. D33 (1986) 1847.

[62] G. Höhler: Sixth International Symposium on Meson-Nucleon Physics and the Structure of the Nucleon, Blaubeuren / Tübingen, Germany July 10-14, 1995.

[63] J.F. Donoghue, B.R. Holstein and Y.C.Lin, Phys. Rev. D37 (1988) 2423.

[64] J. Bijnens and F. Cornet, Nucl. Phys. B296 (1988) 557.

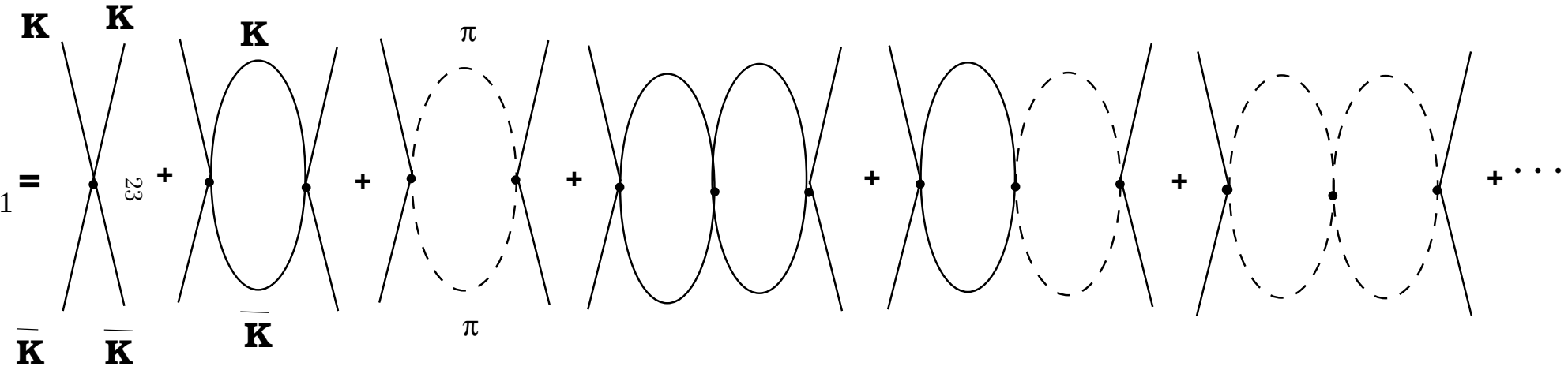
K
K
K
π
1
=
23
+
+
+
+
+
+
+ · · ·
K
K
π

s
I
IV
I=0,(2m$_\pi$)^2
(2m$_K$)^2
I=1,(m$_\pi$+m$_\eta$)^2
II
III

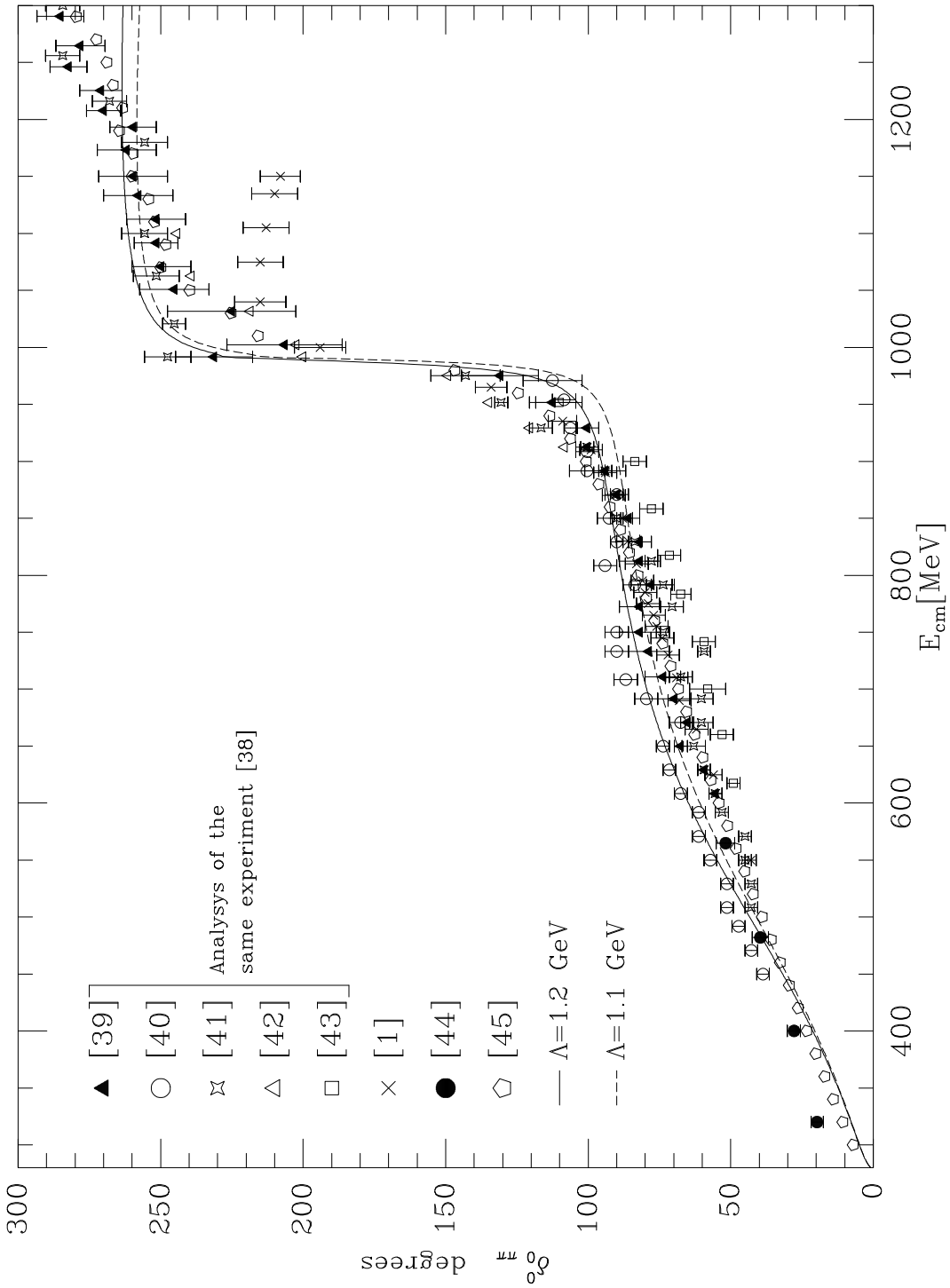
300
250
200
150
100
50
0
400
600
800
1000
1200
E_{cm}[MeV]
$\delta^0_{\pi\pi}$ degrees
[39]
[40]
[41]
[42]
[43]
[1]
[44]
[45]
Analysys of the same experiment [38]
Λ=1.2 GeV
Λ=1.1 GeV

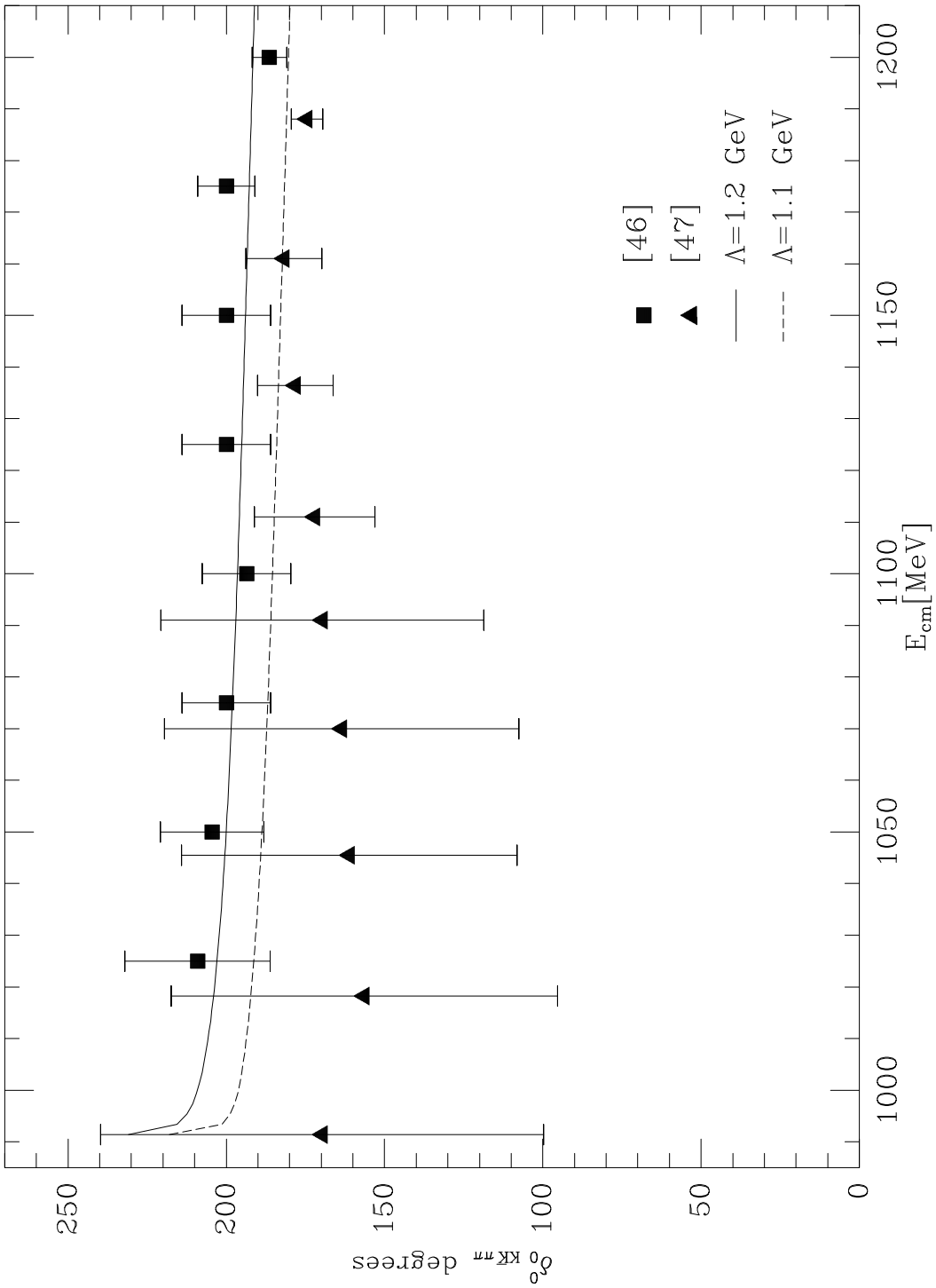
250
200
150
100
50
0
1000
1050
1100
1150
1200
E_{cm}[MeV]
δ^0_0 $K\bar{K}\pi\pi$ degrees
[46]
[47]
Λ=1.2 GeV
Λ=1.1 GeV

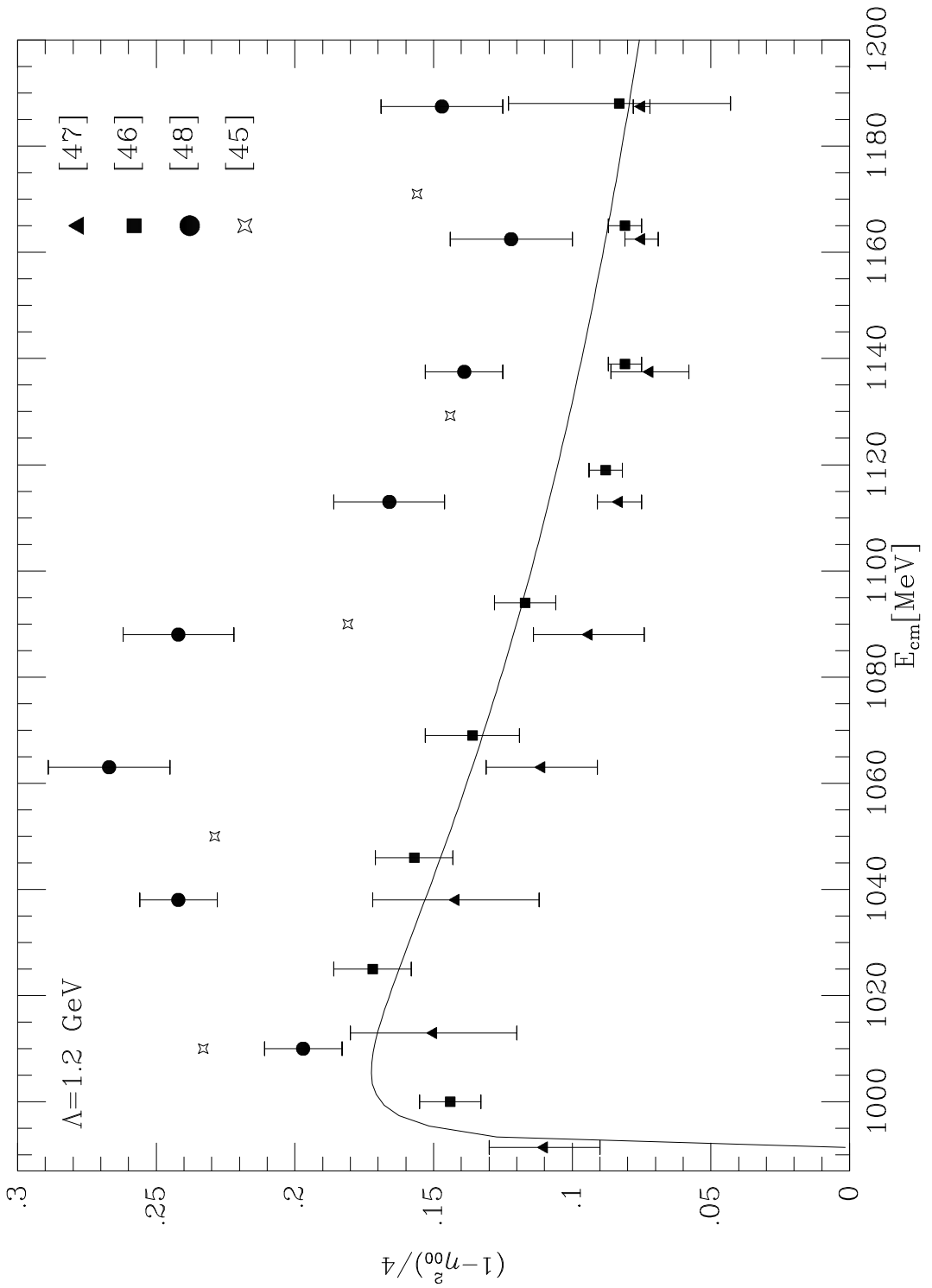
[47]
[46]
[48]
[45]
Λ=1.2 GeV
$(1-\eta_{00}^2)/4$
E_{cm}[MeV]
0
.05
.1
.15
.2
.25
.3
1000
1020
1040
1060
1080
1100
1120
1140
1160
1180
1200

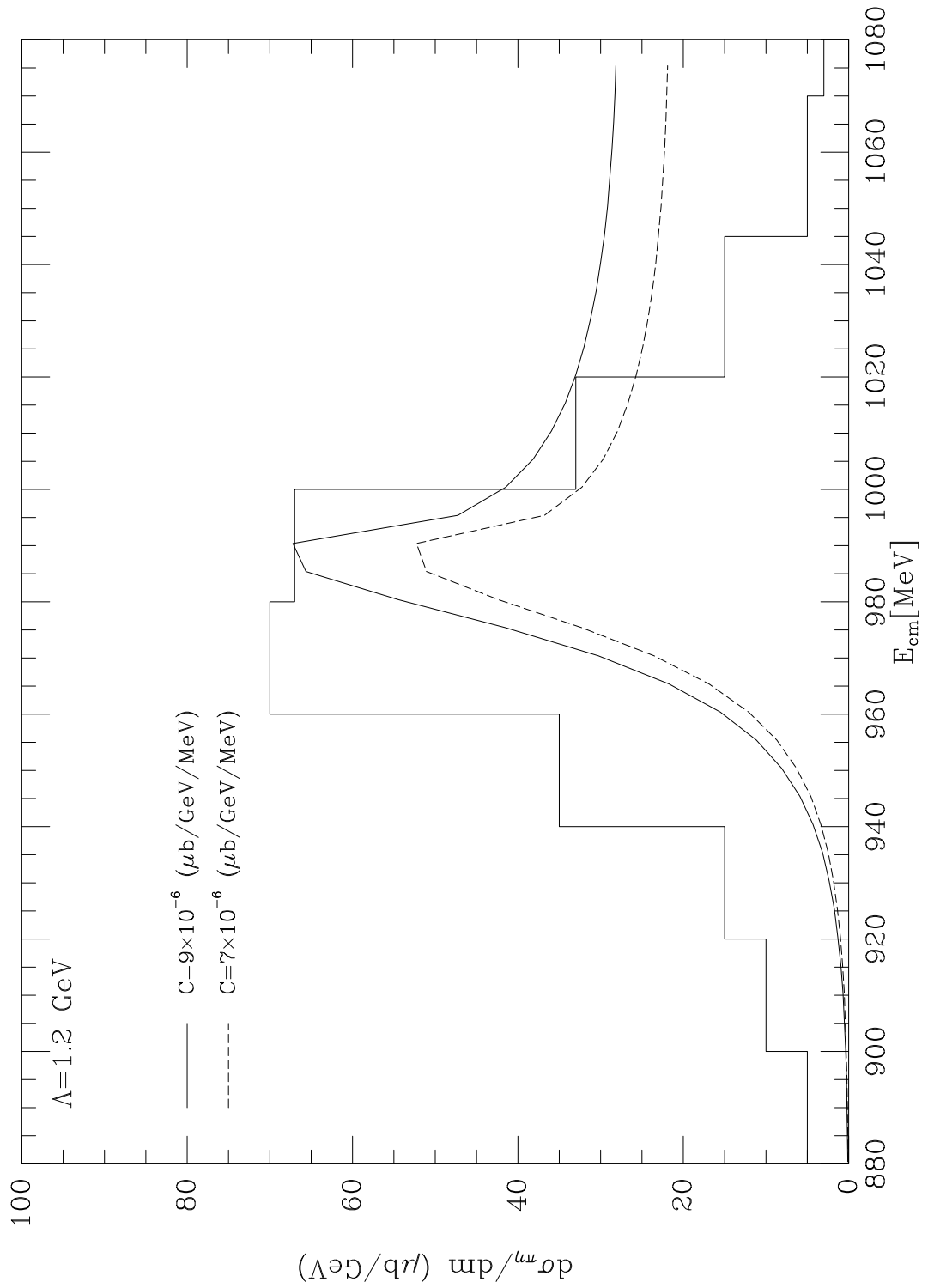
$d\sigma_{\pi\eta}/dm$ (μb/GeV)
E_{cm}[MeV]
Λ=1.2 GeV
C=9×10^{-6} (μb/GeV/MeV)
C=7×10^{-6} (μb/GeV/MeV)
0
20
40
60
80
100
880
900
920
940
960
980
1000
1020
1040
1060
1080

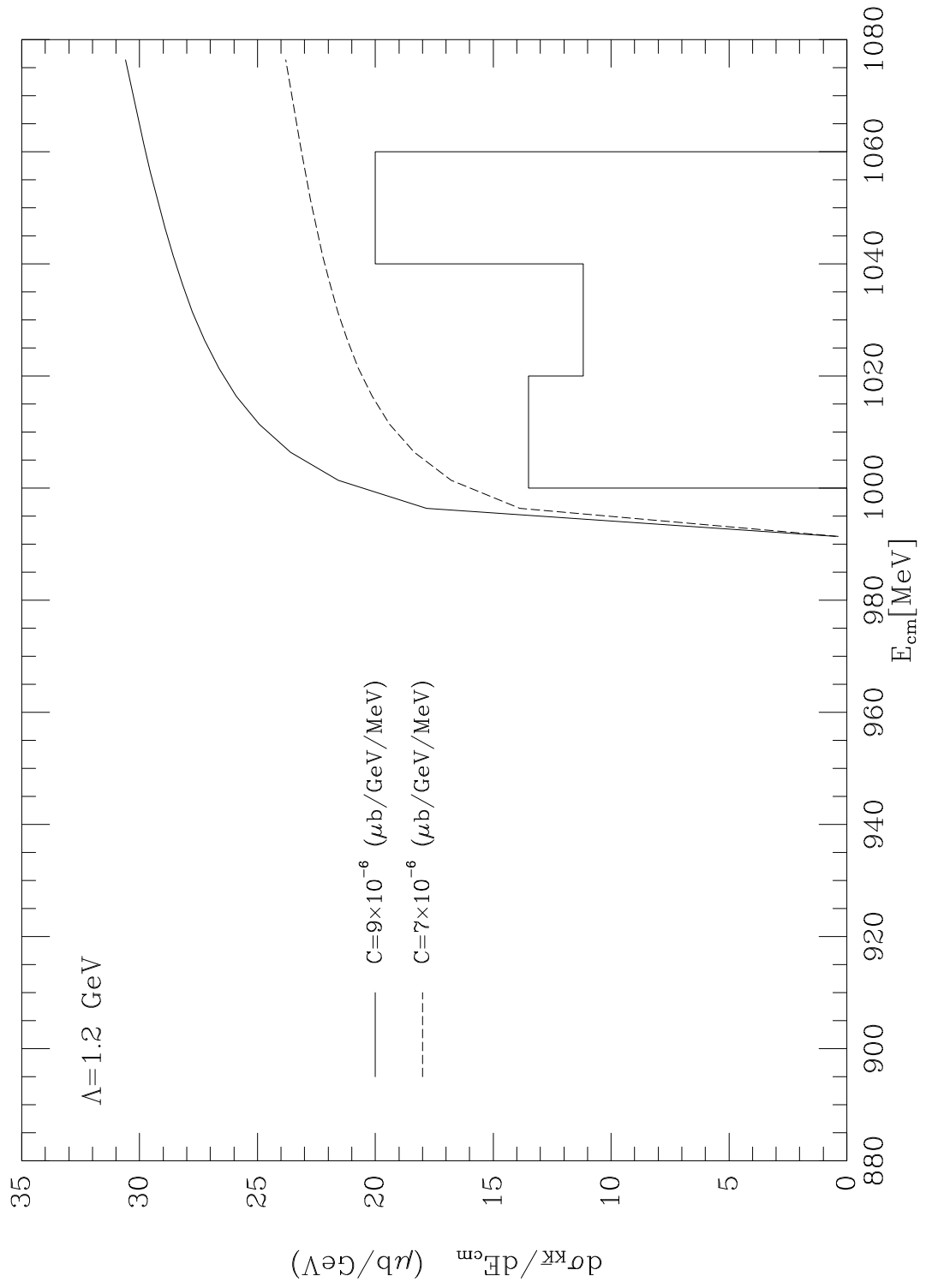
Λ=1.2 GeV
C=9×10^{-6} (μb/GeV/MeV)
C=7×10^{-6} (μb/GeV/MeV)
$d\sigma_{K\bar{K}}/dE_{cm}$ (μb/GeV)
E_{cm}[MeV]
0
5
10
15
20
25
30
35
880
900
920
940
960
980
1000
1020
1040
1060
1080

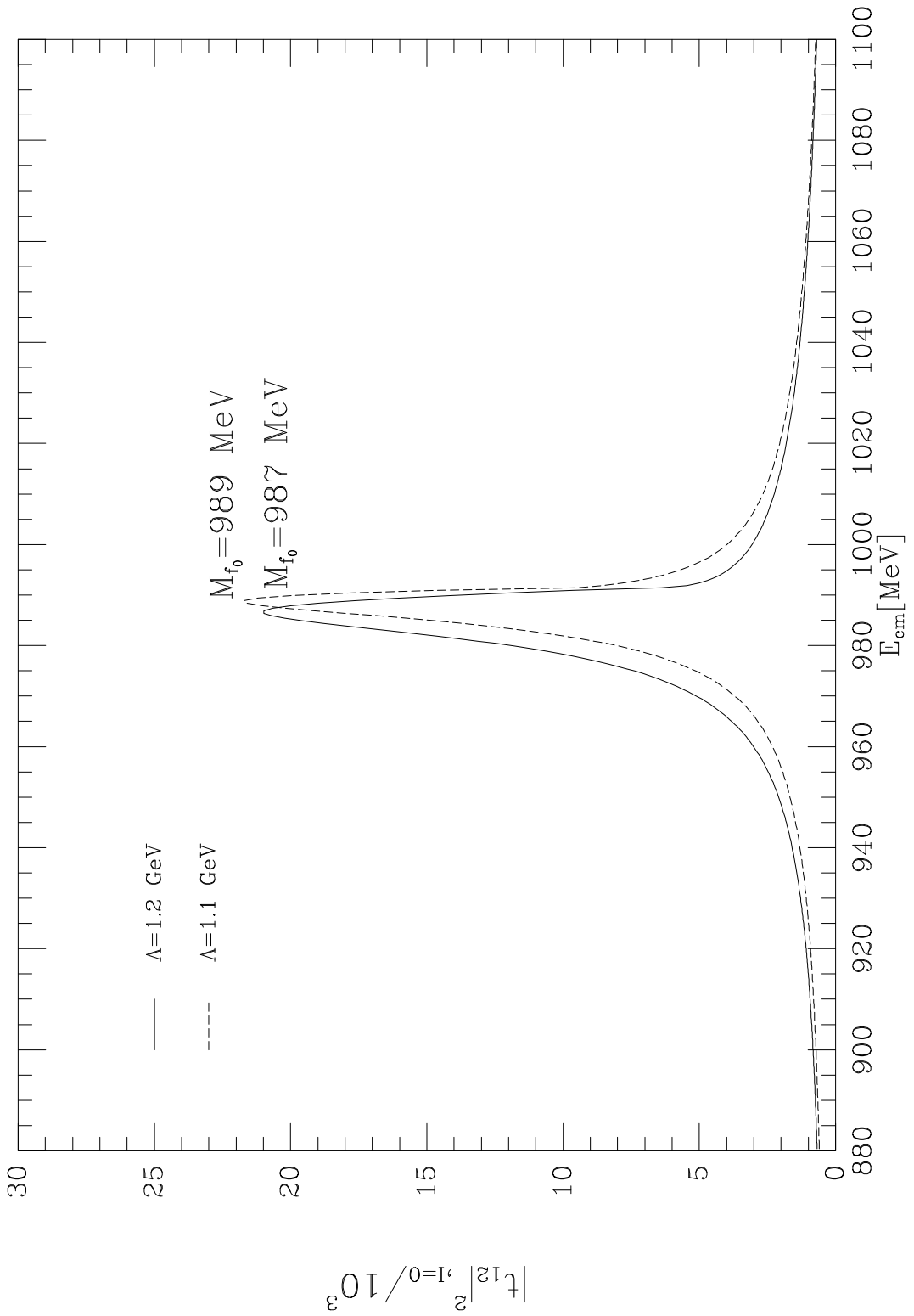
$|t_{I2}|^2_{,I=0}/10^3$
30
25
20
15
10
5
0
880
900
920
940
960
980
1000
1020
1040
1060
1080
1100
E_{cm}[MeV]
M_{f_0}=989 MeV
M_{f_0}=987 MeV
Λ=1.2 GeV
Λ=1.1 GeV

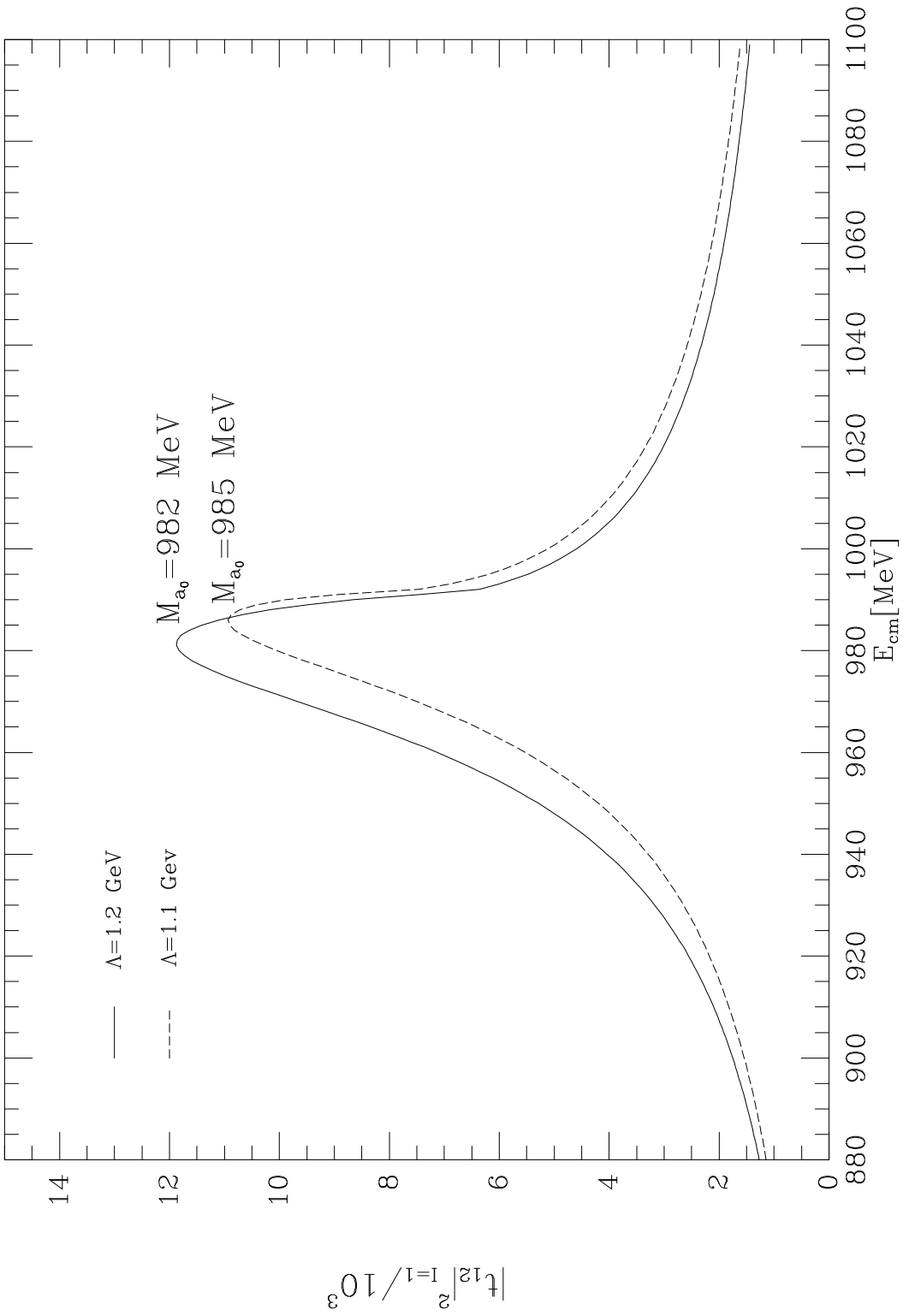
$|t_{12}|^2_{I=1}/10^3$
14
12
10
8
6
4
2
0
880
900
920
940
960
980
1000
1020
1040
1060
1080
1100
E_{cm}[MeV]
M_{a_0}=982 MeV
M_{a_0}=985 MeV
Λ=1.2 GeV
Λ=1.1 Gev